

# Preparation of dense $\beta$ -CaSiO<sub>3</sub> ceramic with high mechanical strength and HAp formation ability in simulated body fluid

L.H. Long<sup>a,c</sup>, L.D. Chen<sup>a,\*</sup>, S.Q. Bai<sup>a</sup>, J. Chang<sup>b</sup>, K.L. Lin<sup>b</sup>

<sup>a</sup> State Key Laboratory of High Performance Ceramics and Superfine Microstructure, Shanghai Institute of Ceramics, Chinese Academy of Sciences, Shanghai 200050, China

<sup>b</sup> Biomaterials and Tissue Engineering Research Center, Shanghai Institute of Ceramics, Chinese Academy of Sciences, Shanghai 200050, China

<sup>c</sup> Graduate School of Chinese Academy of Science, Shanghai 200050, China

Received 29 October 2004; received in revised form 1 March 2005; accepted 12 March 2005

Available online 31 May 2005

## Abstract

In present study, dense CaSiO<sub>3</sub> (CS) ceramics have been fabricated through spark plasma sintering (SPS) technique using  $\beta$ -CS powder prepared by chemical precipitation method. The  $\beta$ -CS ceramic sintered at 950 °C has a relative density of about 95% and shows a fine microstructure with an average grain size of 0.6  $\mu$ m, thus expresses good bending strength of about 294 MPa. The simulated body fluid (SBF) immersion tests show that the dense  $\beta$ -CS ceramic has a high hydroxyapatite (HAp) formation rate on its surface. The HAp layer formed on the CS ceramic surface has a granular structure consisting of silkworm-like HAp grains, and the thickness of HAp and Si-rich layer are 70 and 120  $\mu$ m, respectively.

© 2005 Published by Elsevier Ltd.

**Keywords:** Powders-chemical preparation; Grain size; Mechanical properties; Biomedical applications; Spark plasma sintering; Apatite; CaSiO<sub>3</sub>

## 1. Introduction

Since the discovery of Bioglass® by Hench et al. in the early 1970s, many man-made materials such as glasses, glass-ceramics, ceramics and composites have been found to bond with living bone or living tissue.<sup>1–6</sup> Although these man-made bioactive materials are expected to be used as artificial bone, their practical applications as implants are still greatly restricted because of their poor mechanical properties. CS is one of the promising bioactive materials due to its outstanding bioactivity, which has been revealed by recent studies<sup>7–12</sup>; however, the mechanical properties of the CS are not satisfied because of its low density. The relative densities of the sintered  $\beta$ -CS (low-temperature phase) and  $\alpha$ -CS (high-temperature phase) reported up to date are below 90% and the bending strengths are lower than 70 MPa.<sup>13–16</sup> Difficulties in preparing dense CS ceramic with improved

mechanical properties might limit its potential application as bioactive implants.

Recently, a new rapid sintering technique so-called spark plasma sintering (SPS) has been developed and attracted much attention as a means of enhancing the densification of poorly sinterable materials.<sup>17–20</sup> SPS process is similar to the conventional hot pressing, and the precursors are loaded in a graphite die with a uniaxial pressure during sintering process. However, a pulsed direct current passes through the die and or the sample. This implies that the die or the sample themselves acts as a heating source. The simplified schematic drawing of SPS is shown in Fig. 1. This process has the advantage to provide high heating rate and thus to suppress grain growth and maintain a high densification driving force up to high temperature. There have been many biomaterials prepared by spark plasma sintering.<sup>21–24</sup> For instance, dense HAp bioceramics and HAp–ZrO<sub>2</sub> ceramic composites have been successfully fabricated by using SPS technique, in which the decomposition of HAp and the loss of water have been prevented under a lower sintering temperature and very short processing time.<sup>22</sup>

\* Corresponding author. Fax: +86 21 52413122.

E-mail address: [cld@mail.sic.ac.cn](mailto:cld@mail.sic.ac.cn) (L.D. Chen).

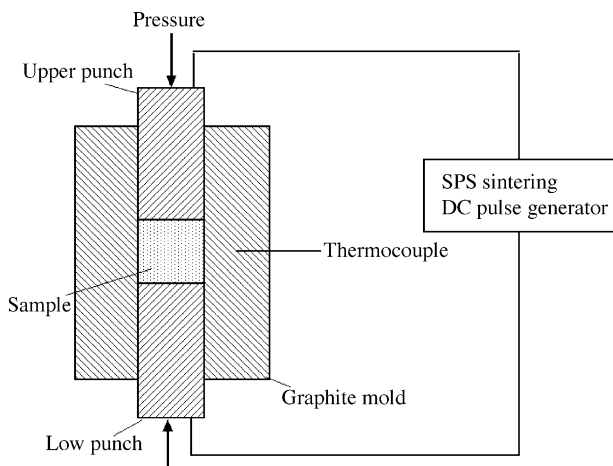


Fig. 1. Schematic drawing illustrating the features of an SPS apparatus.

Other reports showed that SPS-sintered HAp ceramics had better bioactivity than those sintered by hot-pressing.<sup>25</sup>

Herein, we reported the successful preparation of dense CS ceramics by SPS. The microstructures of obtained specimens were analyzed. The mechanical properties were measured and the bioactivity of  $\beta$ -CS ceramics was evaluated with soaking in the simulated body fluid (SBF) solution for various periods.

## 2. Experimental procedure

$\beta$ -CS powder was prepared through a chemical precipitation method using reagent-grade calcium nitrate ( $\text{Ca}(\text{NO}_3)_4 \cdot 4\text{H}_2\text{O}$ ) and reagent-grade sodium silicate ( $\text{Na}_2\text{SiO}_3 \cdot 9\text{H}_2\text{O}$ ) as raw materials. Sodium silicate was dissolved in de-ionized water and the pH value of the solution was adjusted to about 12 using  $\text{NH}_4\text{OH}$ . The obtained  $\text{Na}_2\text{SiO}_3$  solution was dropped into calcium nitrate solution with vigorous agitation. The reactant mixture was filtered, and then washed by de-ionized water and ethanol. The powder was dried at  $80^\circ\text{C}$  and then calcined at  $800^\circ\text{C}$  for 2 h. The obtained powder was  $\beta$ -CS with an average particle size of about  $0.5\ \mu\text{m}$  and the relative density of obtained powder was 99.8% measured by bottle method.

CS powder was put into a graphite die (30 mm in diameter) and was sintered using spark plasma sintering (Dr Sinter 2040, Sumitomo Coal Mining Co.) in a vacuum (less than  $10^{-5}\ \text{Pa}$ ) under a pressure of 40 MPa. The heating rate was  $150\text{--}200^\circ\text{C}/\text{min}$  and dwelling time is 5 min.

The crystalline phases of the as-precipitated powder and sintered specimen were analyzed by XRD (D/max 2200PC, Rigaku, Tokyo, Japan). The density was determined according to Archimedes principle. Microstructures were observed by field emission scanning electron microscope (FE-SEM, JSM-6700F, JEOL, Japan). The distribution of elements was analyzed by electron probe microanalyzer (EPMA, EPMA-8705QH<sub>2</sub>, Shimadzu, Japan). The three-point bending strength of the sintered samples was measured at the mechanical testing machine with a loading rate of  $0.5\ \text{mm}/\text{min}$  according to the JIS R1601 standard (Shimadzu AG-5KN, Japan). A span length of 20 mm and rectangular-prism-shaped specimens ( $3\ \text{mm} \times 4\ \text{mm}$ ) with surface polished by  $0.5\ \mu\text{m}$  diamond powders were used. The fracture toughness,  $K_{\text{IC}}$ , was evaluated by the single-edge notch beam method (Instron-1195, notch width: 0.25 mm, notch depth: 2 mm). In the study, five samples were used to test the average mechanical strength.

In order to evaluate the bioactivity of sintered ceramics, the  $\beta$ -CS sintered at  $950^\circ\text{C}$  were soaked in SBF, which was prepared by dissolving reagent-grade  $\text{CaCl}_2$ ,  $\text{K}_2\text{HPO}_4 \cdot 3\text{H}_2\text{O}$ ,  $\text{NaCl}$ ,  $\text{KCl}$ ,  $\text{MgCl}_2 \cdot 6\text{H}_2\text{O}$ ,  $\text{NaHCO}_3$  and  $\text{Na}_2\text{SO}_4$  in de-ionized water and adjusting the ion concentrations to be similar to those in human blood plasma at  $36.5^\circ\text{C}$ . The SBF was buffered at pH value of 7.40 with trishydroxymethylamine methane [ $(\text{CH}_2\text{OH})_3\text{CNH}_2$ ] and appropriate amount of 1.0 M hydrochloric acid (HCl), as shown in Table 1.<sup>26</sup> The soaking periods were 1, 3, 7, 14, 21 days and SBF was renewed every day. The temperature was maintained at  $36.5^\circ\text{C}$ .

## 3. Results and discussions

### 3.1. $\text{CaSiO}_3$ ceramics and their properties

Fig. 2 shows the X-ray diffraction spectra of the as-prepared powder and bulk ceramics sintered at different temperatures. All the sintered bodies show the same crystal structure ( $\beta$ -CS) as the starting powder below  $950^\circ\text{C}$ , while it changed into  $\alpha$ -CS ceramic at  $970^\circ\text{C}$ . The measured density and mechanical properties of the obtained materials are listed in Table 2. From Table 2, it can be seen that the relative density of the  $\beta$ -CS ceramic sintered by SPS at  $900^\circ\text{C}$  reached 92%. It reached maximum relative density of 95% and the sample still kept low-temperature phase ( $\beta$ -CS). The obtained density of  $\beta$ -CS ceramics was much higher than reported.<sup>16</sup> When the temperature increased to  $970^\circ\text{C}$ , the

Table 1  
Ion concentration of SBF in comparison with human blood plasma

	Concentration (mM)							
	$\text{Na}^+$	$\text{K}^+$	$\text{Ca}^{2+}$	$\text{Mg}^{2+}$	$\text{HCO}_3^-$	$\text{Cl}^-$	$\text{HPO}_4^{2-}$	$\text{SO}_4^{2-}$
SBF	142.0	5.0	2.5	1.5	4.2	148.5	1.0	0.5
Blood plasma	142.0	5.0	2.5	1.5	27.0	103.0	1.0	0.5

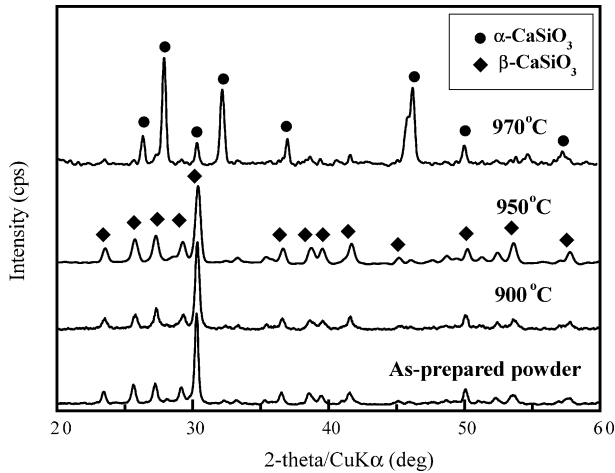


Fig. 2. XRD patterns of  $\beta$ -CaSiO<sub>3</sub> powder and ceramics sintered at different temperatures.

SPS-sintered ceramic almost reached its theoretical density, being more denser than the fabricated by other methods previously reported.<sup>13–15</sup> However, the sample sintered at 970 °C changed into high-temperature phase ( $\alpha$ -CS) completely. The

Table 2

The measured density and mechanical properties of the obtained materials

Temperature (°C)	Relative density (%)	Fracture strength $\sigma_f$ (MPa)	Fracture toughness $K_{Ic}$ (MPa m <sup>1/2</sup> )	Young's modulus (GPa)
900	92	260 ± 16	1.7 ± 0.3	40.4 ± 6.9
950	95	294 ± 11	2.0 ± 0.1	46.5 ± 5.0
970	99	65 ± 5	0.5 ± 0.2	52 ± 4.0

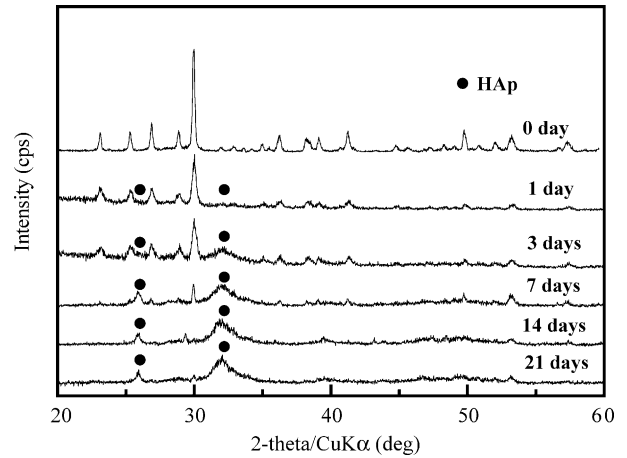


Fig. 4. XRD patterns of the  $\beta$ -CaSiO<sub>3</sub> ceramics soaked in SBF solution for various periods.

bending strength of  $\beta$ -CS sintered at 950 °C was 294 MPa, which was four times more than those reported and much higher than that of HAp ceramics. However, it decreased greatly when the sample changed into  $\alpha$ -CS ceramics.

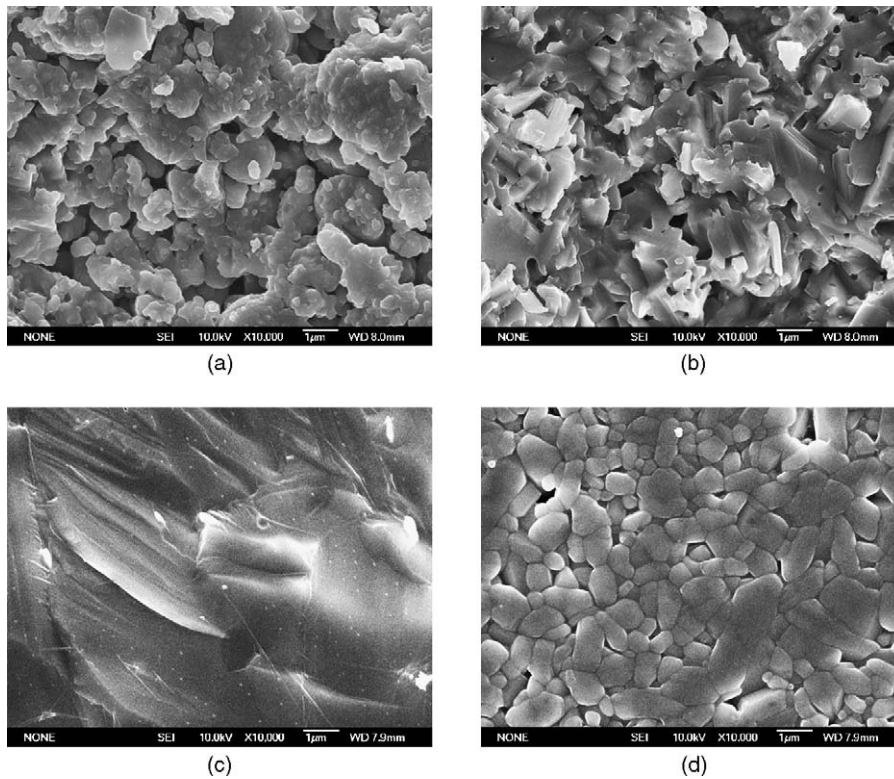


Fig. 3. SEM photographs of fracture and thermally etched surface of  $\beta$ -CaSiO<sub>3</sub> SPS-sintered at various temperatures, (a) 900, (b) 950, (c) 970 and (d) 950 °C thermally etched surface.

Fig. 3 shows the SEM micrographs of fracture surfaces sintered at different temperature and thermally etched surface at 1000 °C in air. The grains were packed loosely at 900 °C (Fig. 3a). However, the  $\beta$ -CS ceramic was completely sintered at 950 °C with an average grain size of 0.6  $\mu\text{m}$  (Fig. 3b and d), similar to the starting powder. These indicated that the mechanisms at 900 and 950 °C were much different. Since

surface diffusion was predominant for the former, it was difficult for the samples to be sintered in a short time; however, the main mechanisms were grain boundary and volume diffusion at 950 °C, which made the sample sintered completely. As well known, SPS was a rapid consolidation technique. In our study, we heated at a rate of around 200 °C/min, which made it possible for the sample to skip over the low-temperature

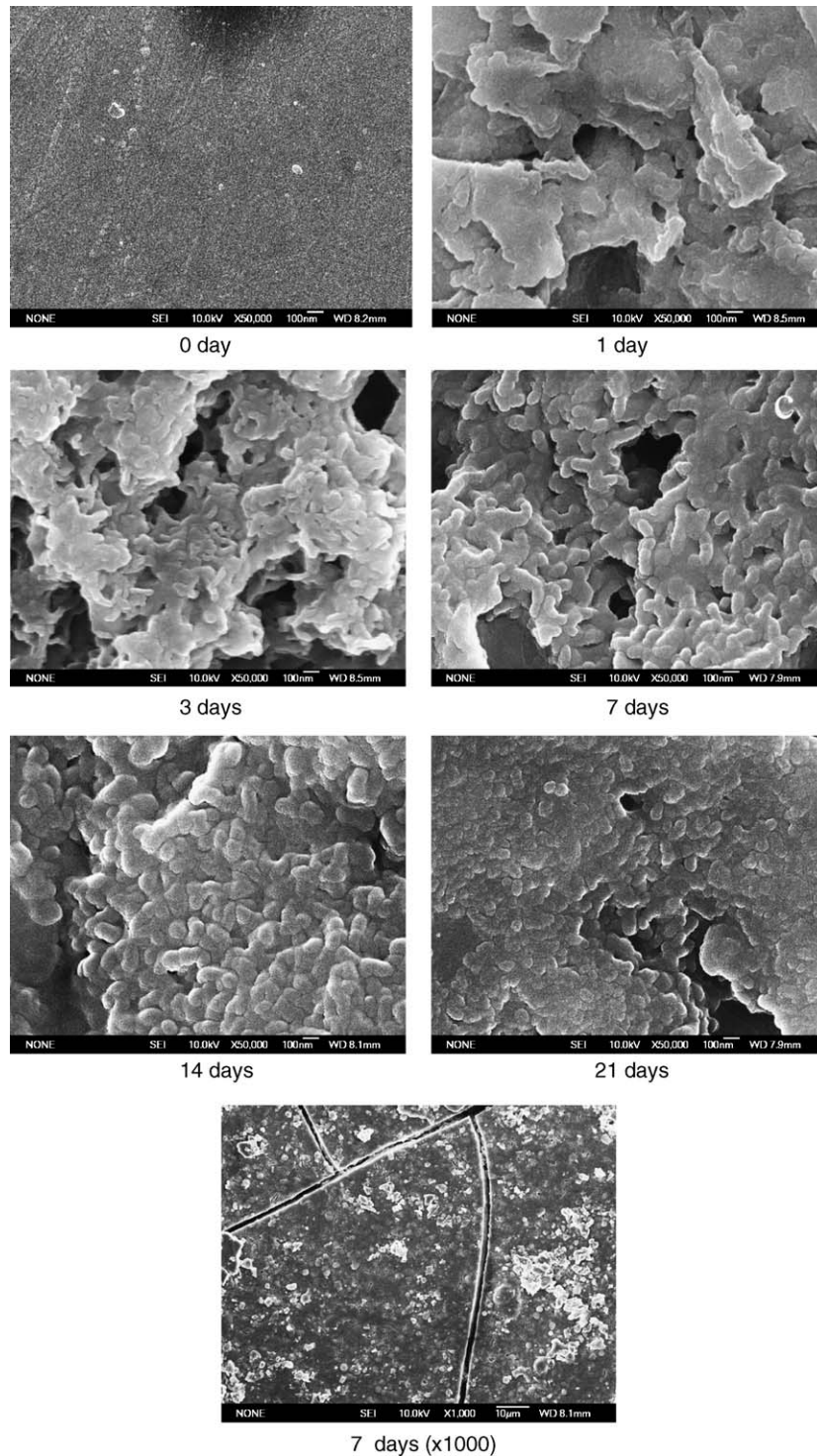


Fig. 5. Surface SEM photographs of  $\beta$ -CaSiO<sub>3</sub> ceramics soaked in SBF solution for various periods.

regime where the surface diffusion was predominant and the grain growth in the low-temperature region was suppressed.<sup>27</sup> In addition, the sample during SPS processing was under an electrical field and the weak current. They could activate the surface of grains and clean the surface of the powder particles, creating various types of surface defects that enhance the grain boundary diffusion.<sup>28,29</sup> Finally, the axial pressure in SPS process also acted as an important role in fabricating dense CS ceramics. All these factors made the  $\beta$ -CS densify rapidly and kept small grain sizes. The process of phase transform improved the densification of  $\alpha$ -CS ceramics nearly to its theoretical density. However, it also made the crystal grains grow rapidly (Fig. 3c). The abnormal grain growth caused great decrease of the mechanical strengths.

### 3.2. SBF immersion tests

The samples sintered at 950 °C for 5 min were immersed in SBF to evaluate its bioactivity. Fig. 4 shows the thin film-XRD patterns of the CS ceramics soaked for different periods. The broad diffraction peaks ( $2\theta = 26$  and  $32^\circ$ ) of HAp were observed in the XRD patterns after soaking for 3 days. The main peaks of HAp became more pronounced with prolonged immersion time due to the growth of the crystalline HAp. After soaking for 7 days, the diffraction peaks of HAp became main component in the XRD pattern and the diffraction peaks of  $\beta$ -CS became very weak, which revealed that HAp had covered the surface of the specimen. When the soaking time is more than 14 days, the peaks of CS disappeared completely.

Fig. 5 shows the surface morphologies of the  $\beta$ -CS ceramic immersed in SBF for 0, 1, 3, 7, 14, 21 days. The surface of the sample immersed in SBF for 1 day became coarser, as compared to the starting state, which may be caused by the dissolution of Ca and Si.<sup>7,10</sup> A few granular crystals were also found on the surface of sample soaked for 1 day. After 3 days immersion, the surface of the sample was almost covered by the silkworm-like HAp particles, and their diameter was 50 nm and length was 200–300 nm. After soaking for 7

Table 3

The Ca/P molar ratio of the obtained materials soaked in SBF solution for various periods

Time (day)	Ca/P (molar)
1	32.5
3	1.95
7	1.70
14	1.68
21	1.66

days, the amount of HAp particles increased significantly on the surface and the HAp layers became much denser after soaking for 14 and 21 days. Caused by the desiccation and dehydration, cracks in the HAp layer on the surface were observed for the sample soaked for more than 7 days.

The surface of the  $\beta$ -CS ceramics after soaking was analyzed by electron probe microanalyzer (EPMA). After soaking for 1 day, Si and Ca were the main components at the specimen surface and P element did not appear apparently in the spectrum. The intensity of Si peak decreased greatly, and that of P increased quickly with the increase of the soaking time. No Si peaks were detected. The Ca/P molar ratio was also analyzed for all the samples. It increased with immersion time and reached about 1.67 for the sample soaked for 7 days (Table 3.), showing the deposition of HAp layer. These results are consistent with the results of XRD analysis and SEM observation.

The SEM images and the element distribution of the polished cross-section of CS ceramics by EPMA are shown in Fig. 6. For the sample soaked for 3 days, the thickness of silica-rich layer reached about 40  $\mu\text{m}$ , and the thickness of HAp layer was about 10  $\mu\text{m}$  (Fig. 6a). After soaking for 7 days, the thickness of the silica-rich layer and HAp layer increased to 120 and 70  $\mu\text{m}$ , respectively. The growth of the HAp layer on the  $\beta$ -CS ceramic surface obtained in the present experiment is much quicker than those previously reported.<sup>14</sup> The higher growth rate might be attributed to the fine grain in the SPS-sintered  $\beta$ -CS, and the deficiency such

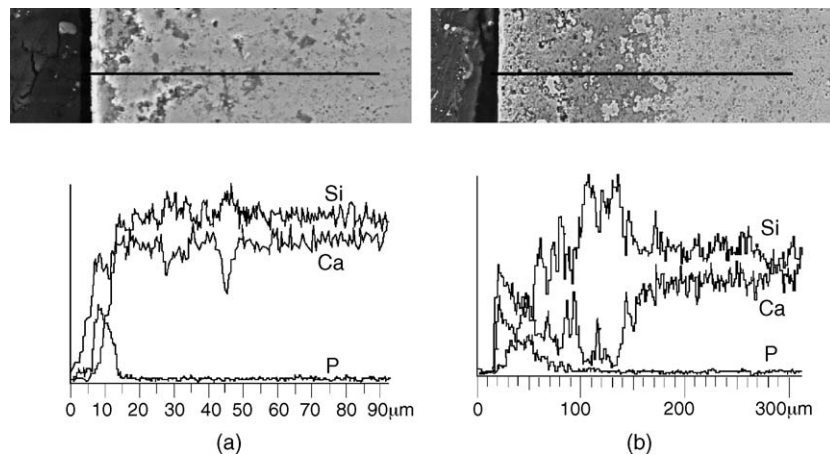


Fig. 6. SEM images and element distribution in EPMA line-scanning analysis of the polished cross-section of  $\beta$ -CaSiO<sub>3</sub> ceramics soaked in SBF for 3 days (a) and 7 days (b).

as  $\text{Ca}^{2+}$  ion caused by electric field or weak current through samples.

#### 4. Conclusions

The SPS process could fabricate dense CS ceramics rapidly and suppress the grain growth effectively. Dense CS ceramics were successfully fabricated at a low temperature and short dwelling time of 5 min. The maximum bending strength of 294 MPa was achieved for the sample sintered at 950 °C. SBF soaking results revealed that the SPS-sintered  $\beta$ -CS showed good bioactivity with a larger growth rate of HAp layer on its surface. The dense  $\beta$ -CS ceramics sintered by SPS might be potential candidate as bioactive implant materials.

#### Acknowledgement

This work is supported by National Natural Science Foundation of China under grant No. 50232020 and 50325208.

#### References

- Gross, U., Kinne, R., Schmitz, H. J. and Strunz, V., The response of bone to surface active glass/glass-ceramics. *CRC. Crit. Rev. Biocompat.*, 1993, **4**, 2.
- Hench, L. L. and Anderson, O., Bioactive glass. In *An Introduction to Bioceramics*, ed. Larry L. Hench and June Wilson. World Scientific, Singapore, 1993, pp. 41–62.
- Cao, W. P. and Hench, L. L., Bioactive materials. *Ceram. Int.*, 1996, **22**, 493–507.
- Wang, M., Develop bioactive composite materials for tissue replacement. *Biomaterials*, 2003, **24**, 2133–2151.
- Lopes, M. A., Knowles, J. C. and Santos, J. D., Structural insights of glass-reinforced hydroxyapatite composites by rictveld repinement. *Biomaterials*, 2000, **21**, 1905–1910.
- Habiovic, P., Barrère, F., Van Blitterswijk, C., De Groot, K. and Layrolle, P., Biominetic hydroxyapatite coating on metal implants. *J. Am. Ceram. Soc.*, 2002, **85**, 517–522.
- Aza, P. N. D. E., Luklinska, Z. B., Anseau, M., Guitian, F. and De Aza, S., Morphological studies of pseudowollastonite for biomedical application. *J. Microscopy*, 1996, **182**, 24–31.
- Siriphannon, P., Kameshima, Y., Yasumori, A., Okada, K. and Hayashi, S., Formation of hydroxyapatite on  $\text{CaSiO}_3$  powders in simulated body fluid. *J. Eur. Ceram. Soc.*, 2002, **22**, 511–520.
- Liu, X. Y., Zheng, X. B. and Ding, C. X., Apatite formed on the surface of plasma-sprayed wollastonite coating immersed in simulated body fluid. *Biomaterials*, 2001, **22**, 2007–2012.
- Liu, X. Y., Ding, C. X. and Chu, P. K., Mechanism of apatite formation on wollastonite coatings in simulated body fluids. *Biomaterials*, 2004, **25**, 1755–1761.
- De Aza, P. N., Luklinska, Z. B., Anseau, M. R., Guitian, F. and De Aza, A., Bioactivity of pseudowollastonite in human saliva. *J. Dent.*, 1999, **27**, 107–113.
- Dufrane, D., Delloye, C., Mckay, I. J., De Aza, S., De Aza, P. N., Schneider, X. J. et al., Indirect cytotoxicity evaluation of pseudowollastonite. *J. Mater. Sci: Mater. Med.*, 2003, **14**, 33–38.
- Hayashi, S., Okada, K. and Otsuka, N., Preparation of  $\text{CaSiO}_3$  powder by coprecipitation method and their sinterability. *J. Ceram. Soc. Jpn.*, 1991, **12**, 1224–1227.
- Siriphannon, P., Hayashi, S., Yasumori, A. and Okada, K., Preparation and sintering of  $\text{CaSiO}_3$  from coprecipitated powder using NaOH as precipitant and its apatite formation in simulated body fluid solution. *J. Mater. Res.*, 1999, **14**, 529–536.
- Siriphannon, P., Kameshima, Y., Yasumori, A., Okada, K. and Hayashi, S., Influence of preparation conditions on the microstructure and bioactivity of  $\alpha$ - $\text{CaSiO}_3$  ceramics: Formation of hydroxyapatite in simulated body fluid. *J. Biomed. Mater. Res.*, 2000, **52**, 30–39.
- Endo, T., Sugiur, A., Sakamaki, M., Takizwa, H. and Shimada, M., Sintering and mechanical properties of  $\beta$ -wollastonite. *J. Mater. Sci.*, 1994, **29**, 1056–1504.
- Hong, J. S., De la Torre, S. D., Gao, L., Miamoto, K. and Hiymoto, H., Bending strength and microstructure of  $\text{Al}_2\text{O}_3$  ceramics densified by spark plasma sintering. *J. Eur. Ceram. Soc.*, 2002, **20**, 2149–2152.
- Wang, S. W., Chen, L. D. and Hirai, T., Densification of  $\text{Al}_2\text{O}_3$  powder using spark plasma sintering. *J. Mater. Res.*, 2000, **15**, 982–987.
- Hong, J. S., De, La, Torre, S. D., Gao, L., Miyamoto, F. and Miyamoto, H., Synthesis and mechanical properties of  $\text{ZrO}_2/\text{Al}_2\text{O}_3$  composites prepared by spark plasma sintering. *J. Mater. Lett.*, 1998, **17**, 1313–1315.
- Gao, L., Wang, H. Z., Hong, J. S., Miyamoto, H., Miyamoto, K. and Nishikawa, Y., SiC-ZrO<sub>2</sub>(3Y)-Al<sub>2</sub>O<sub>3</sub> nanocomposites superfast densified by spark plasma sintering. *NanoStruct. Mater.*, 1999, **11**, 43–45.
- Gu, Y. W., Loh, N. H., Khor, K. A., Tor, S. B. and Cheang, P., Spark plasma sintering of hydroxyapatite powders. *Biomaterials*, 2002, **22**, 37–43.
- Shen, Z. J., Adolfsson, E., Nygren, M., Gao, H., Kawaoka, L. and Niihara, K., Dense hydroxyapatite-zirconia ceramic composite with high strength for biological applications. *Adv. Mater.*, 2001, **13**, 214–216.
- Lee, Y. I., Lee, J. H., Hong, S. H. and Kim, D. Y., Preparation of nanostructured TiO<sub>2</sub> ceramics by spark plasma sintering. *Mater. Res. Bull.*, 2003, **38**, 925–930.
- Li, W. and Gao, L., Fabrication of HAp-ZrO<sub>2</sub> (3Y) nano-composite by SPS. *Biomaterials*, 2003, **24**, 937–940.
- Nakahira, A., Tamai, M., Aritani, H., Nakamura, D. and Yamashita, K., Biocompatibility of dense hydroxyapatite prepared using an SPS process. *J. Biomed. Mater. Res.*, 2002, **62**, 550–557.
- Cho, S. B., Nakanishi, K., Kokubo, T. and Soga, N., Dependence of apatite formation on silica gel on its structure: effect of heat treatment. *J. Am. Ceram. Soc.*, 1995, **78**, 1769–1774.
- Harmer, M. P. and Brook, R. J., Fast firing-microstructural benefits. *J. Br. Ceram. Soc.*, 1981, **80**, 147–148.
- Shen, Z. J., Zhao, Z., Peng, H. and Nygren, M., Formation of tough interlocking microstructures in silicon nitride ceramics by dynamic ripening. *Nature*, 2002, **417**, 266–268.
- Shen, Z., Johnsson, M., Zhao, Z. and Nygren, M., Spark plasma sintering of alumina. *J. Am. Ceram. Soc.*, 2002, **85**, 1921–1927.